


Cite this: *RSC Adv.*, 2020, 10, 38063

# Calcium carbonate nanowires: greener biosynthesis and their leishmanicidal activity

Mehrdad Khatami,<sup>ab</sup> Hajar Q. Alijani,<sup>a</sup> Farideh Mousazadeh,<sup>a</sup> Nooshin Hashemi,<sup>c</sup> Zahra Mahmoudi,<sup>c</sup> Samaneh Darijani,<sup>c</sup> Mehdi Bamorovat,<sup>d</sup> Alireza Keyhani,<sup>d</sup> Meghdad Abdollahpour-Alitappeh<sup>e</sup> and Fariba Borhani<sup>\*f</sup>

The synthesis of inorganic rod shape nanostructures is important in chromatography, dentistry, and medical applications such as bone implants, and drug and gene delivery systems. Herein, calcium carbonate ( $\text{CaCO}_3$ ) nanowires were synthesized using a plant extract and the ensuing nanoparticles were characterized by XRD, FESEM, and HR-TEM. Then, the leishmanicidal effects of biogenic calcium carbonate nanowires were investigated against *Leishmania major* including the toxicity of varying concentrations of nanoparticles, and the percentage of viable and apoptotic cells based on flow cytometry analysis. Based on the results, the  $\text{IC}_{50}$  of these polymorphs were calculated to be  $800 \mu\text{g mL}^{-1}$ . An ecofriendly, inexpensive, and novel biogenic method for the production of a new advanced inorganic nanostructure,  $\text{CaCO}_3$  nanowires, is described without using hazardous chemicals; calcium carbonate nanowires maybe used as a smart drug carrier.

Received 20th May 2020

Accepted 28th September 2020

DOI: 10.1039/d0ra04503a

rsc.li/rsc-advances

## 1. Introduction

In recent years, scientists have been scrutinizing the anti-parasitic properties of nanostructures and special effort has been made to treat common human and animal diseases.<sup>1,2</sup> In view of the universal spread of leishmaniasis, and its drug resistance, novel therapeutic nano-medicine approaches are of particular significance.<sup>3,4</sup> So far, various nanoparticles such as  $\text{ZnO}$ ,<sup>5</sup>  $\text{TiO}_2$ ,<sup>6</sup> and  $\text{Au}$ <sup>7</sup> have been studied for their leishmanicidal properties.

$\text{CaCO}_3$  is abundant in nature,<sup>8</sup> and is available in various forms namely, calcite, aragonite, and vaterite.<sup>9</sup> This mineral is formed during the nature's biomineralization process.<sup>10</sup> In recent decades, calcium carbonate nanocomposite has garnered much attention due to their high cell biocompatibility.<sup>11</sup> Although vaterite is the least abundant among polymorphs of calcium carbonate, it is a biologically valuable element in organisms.<sup>12</sup> Vaterite is weak in terms of chemical stability<sup>13</sup> and rapidly gets converted to the calcite form. Different factors like pH, presence of the organic precursor, type

of solvent, and concentration of precursors are effective in transforming the vaterite to calcite form.<sup>14</sup> The calcium carbonate nanoparticles has been widely used due to their widespread applications in engineering,<sup>15</sup> dentistry,<sup>16,17</sup> drug delivery,<sup>18</sup> biotechnology,<sup>19</sup> bone regeneration<sup>20</sup> and environmental protection.<sup>21</sup> The use of calcite nanoparticles has increased significantly because of their pervasive availability, low cost and ease of synthesis,<sup>22</sup> biocompatibility, and the potential for absorption and for bone tissue repairs in the biomedical field. Yu *et al.*<sup>23</sup> have reported excellent potential for calcium carbonate nanostructure scaffolds in bone regeneration. Fujihara *et al.*<sup>24</sup> reported that calcium carbonate nanostructure improved the proliferation of osteoblast cells.

Leishmaniasis is a serious public health concern and the disease comprise 3 typical groups namely visceral leishmaniasis (VL), cutaneous leishmaniasis (CL), and mucocutaneous leishmaniasis (MCL); CL form has the most prevalent rate while Zoonotic CL (ZCL) is caused by *Leishmania (L.) major*. Due to the recent spread of the disease the development of new effective therapies has become a priority for the World Health Organization (WHO).<sup>25–27</sup> Nanotechnology-based strategies using nanoscopic tools is one of the most effective treatment for protozoan infections.<sup>28,29</sup> In the meantime, antibacterial, antivirals, and anti-parasitic properties of nanomaterials have been extensively investigated due to their favorable physicochemical properties.<sup>30–38</sup> So far, the anti-leishmanial activity of various nanomaterials such as silver, zinc oxide, liposomes, titanium oxide has generated positive results but the calcium carbonate nanostructures have not been studied although calcium nanostructure have been considered in various fields due to their

<sup>a</sup>Noncommunicable Diseases Research Center, Bam University of Medical Sciences, Bam, Iran. E-mail: mehrdad7khatami@gmail.com

<sup>b</sup>Cell Therapy and Regenerative Medicine Comprehensive Center, Kerman University of Medical Sciences, Kerman, Iran

<sup>c</sup>School of Medicine, Bam University of Medical Sciences, Bam, Iran

<sup>d</sup>Leishmaniasis Research Center, Kerman University of Medical Sciences, Kerman, Iran

<sup>e</sup>Cellular and Molecular Biology Research Center, Larestan University of Medical Sciences, Larestan, Iran

<sup>f</sup>Medical Ethics and Law Research Center, Shahid Beheshti University of Medical Sciences, Tehran, Iran. E-mail: faribaborhani@msn.com



non-toxicity, suitability for intravenous and oral administration, high biodegradability, and good absorption in the human body.<sup>39</sup>

In view of our ongoing studies exploiting the plant-mediated strategies for the assembly of nanoparticles, the synthesis of calcium carbonate nanowires and their anti-leishmanicidal effects were undertaken; calcium nanowires were synthesized using a plant extract and then, their anti-leishmanicidal effects were examined on *Leishmania major* in *in vitro*.

## 2. Experimental

### 2.1. Materials

All chemicals and reagents were prepared from Merck Chemicals Co. Deionized water (DI) was used at all stages of the experimental work. The plant material used in the synthesis was purchased from a local supermarket.

### 2.2. Green synthesis of calcium carbonates polymorphs

At the outset, the young branches of *Nasturtium officinale* were washed three times with deionized water and were dried at room temperature for 7 days. The plant surface moisture was removed at room temperature then milled to a fine powder by electric Stainless Steel Home Grinding Milling Machine. To *N. officinale* young branches powder (10 g), deionized water (10 mL) was added and shaken on orbital shaker for 24 hours, then centrifuged at 8000 rpm for 15 min and filtered with Whatman filter paper no. 42. A stock solution (200 mL of 0.1 M  $\text{CaCl}_2 \cdot 2\text{H}_2\text{O}$ ) was added drop wise to 100  $\text{cm}^3$  plant extract at 80 °C. The pH of the mixture was raised to 11 by addition of sodium hydroxide solution (1 M); precipitate ensued after increasing the pH. The obtained mixture was stored at room temperature for two hours, then cooled at room temperature, and incubated at 70 °C for 1 day. The resulting nanoparticles were centrifuged and washed with ethanol and DI, respectively, then dried at 120 °C and calcined in the furnace at 600 °C for 5 h.

### 2.3. Physicochemical characterization of nanoparticles

The structure and size of resulting nanoparticles were analyzed by field-emission SEM (FESEM) (Sigma VP, ZEISS) and a high-resolution TEM (HRTEM) (Tecnai, 20FEI). The XRD was recorded on X'PertPro Advance with  $\text{CuK}\alpha$  radiation 1.54 Å at 40 kV and 30 mA. Also, EDAX analysis was performed to determine the purity of the nanoparticles.

### 2.4. Leishmanicidal activity

In this study, the *L. major* culture was treated with varying concentrations of biogenic  $\text{CaCO}_3$  nanowire and amphotericin-B; amphotericin-B has been used to treat fungal infections associated with AIDS, central nervous system (CNS) infections, lung infections, unicellular infections such as VL, *etc.*

Amphotericin and nanoparticles were prepared in DMSO. An adequate amount of promastigotes was prepared by culturing the *L. major* in RPMI 1640 (Gibco) with 20% FCS (Gibco).<sup>20</sup> Promastigote proliferation was measured by MTT [3-(4,5-methylthiazol-2-yl)-2,5-diphenyltetrazolium bromide] assay. About  $3 \times 10^6$  promastigotes of *L. major* per well were cultured in RPMI 1640 (Gibco) and 20% FCS (Gibco) and permitted to multiply for 72 h in the medium (control group), in solvent (other control groups) or the presence of  $\text{CaCO}_3$  NPS in 3 separate 96-well microtiter plates and in concentration of 100, 200, 400 and 800  $\mu\text{g mL}^{-1}$ . Then, 20  $\mu\text{L}$  of tetrazolium (Roche, Germany) (5  $\text{mg mL}^{-1}$ ) was poured to each well and incubated in 18 °C for 4 h to be centrifuged in 1000g for 10 min. The supernatant was removed and 100  $\mu\text{L}$  of DMSO was poured to each well and resuspended. Finally, the ELISA reader was used to read OD at 450 nm.

## 3. Discussion and results

### 3.1. XRD analysis

XRD pattern for  $\text{CaCO}_3$  nanowire obtained by the green method at pH = 11 after calcination at 600 °C is depicted in Fig. 1. According to XRD data, there are two crystalline phases of  $\text{CaCO}_3$  (calcite and vaterite) in the final product. No peak of the

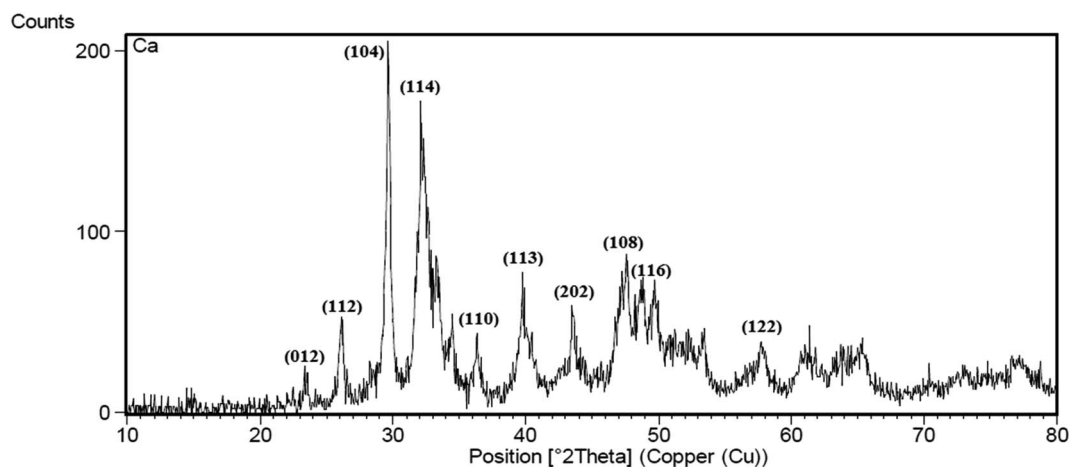


Fig. 1 X-ray diffraction spectrum of  $\text{CaCO}_3$  nanowire synthesis using plant extract.



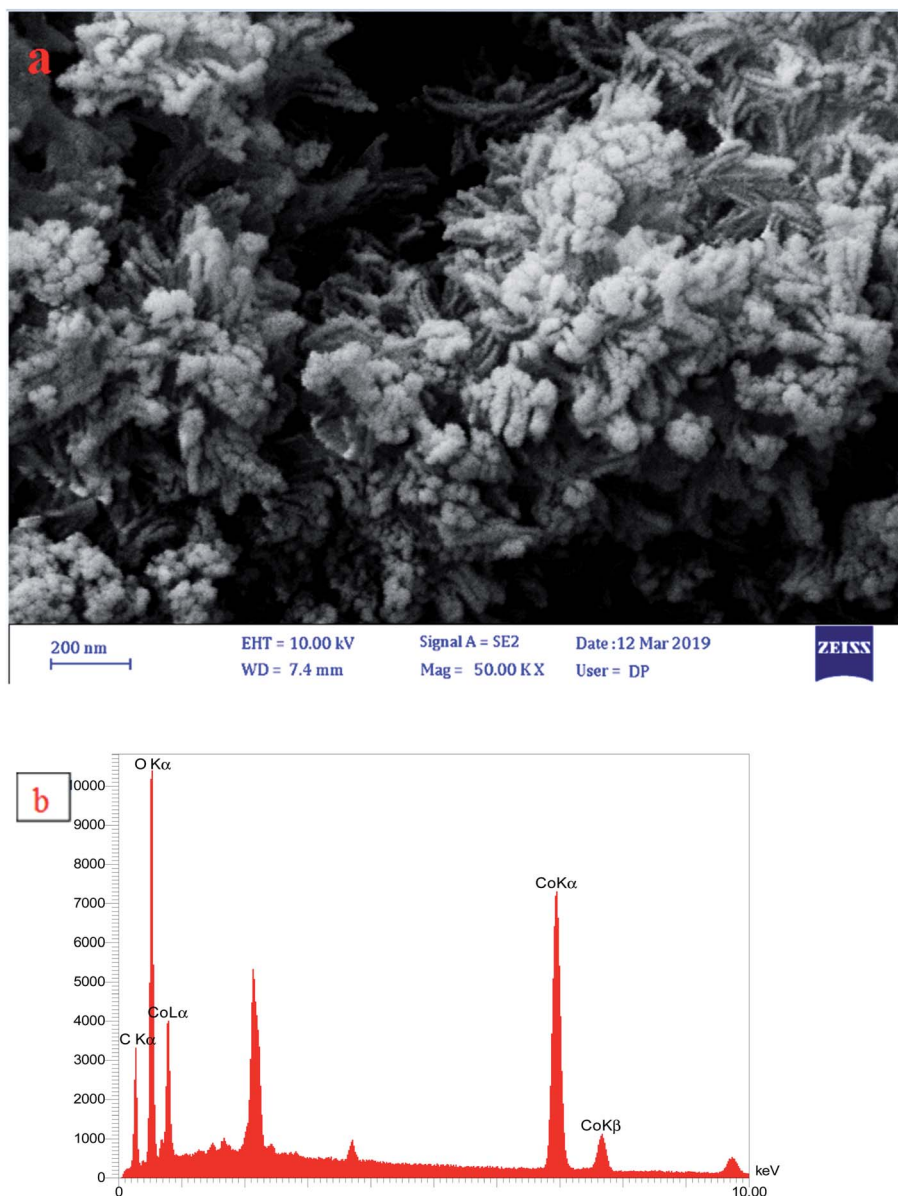


Fig. 2 (a) SEM image of star-like shaped and (b) EDX profile of  $\text{CaCO}_3$  nanostructures.

aragonite crystalline phase was observed in the graph.<sup>40</sup> The peaks observed in  $2\theta = 23, 29.9, 36, 39.5, 47, 48.5, 58, 61, 64, 65.5$  and  $76.50$  related to the presence of calcite phase in the nanowires.<sup>40</sup> Also, the peaks observed in  $2\theta = 26, 32, 33, 34, 43.5, 49$ , and  $53.50$  are the main features of the vaterite phase in the nanowires<sup>41</sup> based on the standard JCPDS (no. 85-1108). These findings are similar to previously published reports on  $\text{CaCO}_3$  nanoparticles that synthesized by using chemical methods.<sup>40–43</sup>

### 3.2. Field-emission scanning electron microscope and energy dispersive spectrometer (EDS)

The morphology of  $\text{CaCO}_3$  nanostructures was investigated by SEM analysis (Fig. 2). The uniform addition of calcium chloride solution to the plant extract in the air and  $\text{CO}_2$  environment for

two hours with a continuous stirring resulted in the formation of calcium carbonate nanoparticles. The addition of the NaOH solution to calcium carbonate particles produced polycrystals of vaterite. The incubation of the mixture resulted in the accumulation of particles and the formation of star-like structures, presumably due to the increase in salt content in a small volume of space. A 50% increase in sodium hydroxide salts reduced the stability of calcium carbonate particles and reduced the number of calcium ions relative to carbonate, resulting in an increase in the number of elliptical particles and the formation of irregular star-like structures.<sup>44</sup> The components of calcium carbonate powders have been calcined at  $600^\circ\text{C}$  are shown in Fig. 2b. The EDX analysis (Fig. 2b) of  $\text{CaCO}_3$  nanoparticles showed that nanoparticles comprise 59.8 (wt%) calcium, 33.4 oxygen, and 6.8 carbon.

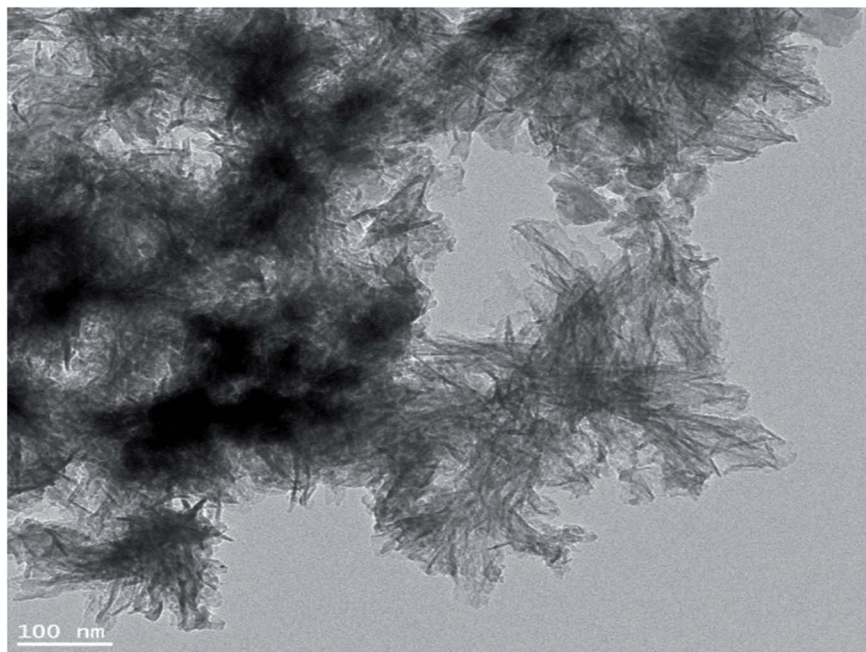


Fig. 3 HRTEM micrographs of  $\text{CaCO}_3$  nanowires.

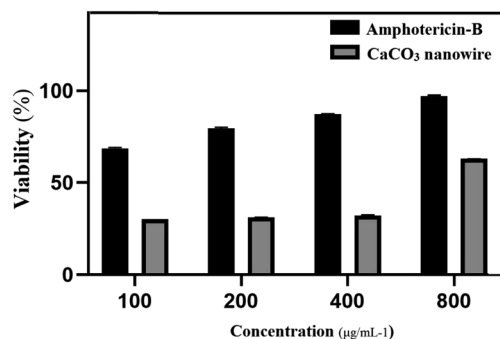


Fig. 4 MTT assay of  $\text{CaCO}_3$  nanowire on *L. major* after 72 h.

### 3.3. HRTEM analysis

Fig. 3 depicts the image of calcium carbonate nanowires<sup>45</sup> and their nanostring like particles (Fig. 3) at pH = 11, respectively. The minimum and maximum sizes of these single crystals are 3 to 76 nm, respectively. Nanowires shape (or needle-like) structures with a full center confirms the precursor conductivity of calcium for the calcite nanoparticles formation.<sup>46</sup>

### 3.4. Leishmanicidal activity of nanowires calcium carbonate nanowires

Leishmanicidal activity of varying concentrations of amphotericin-B was investigated in comparison with the  $\text{CaCO}_3$  nanowire on *L. major* cultures. Fig. 4 shows the toxicity of  $\text{CaCO}_3$  nanowire as compared to the control group after 72 h. The MTT assay was applied to measure the cytotoxic effect of  $\text{CaCO}_3$  on *L. major* promastigotes. Promastigotes growth inhibition of *L. major* were evaluated in the presence of 100, 200, 400, and 800  $\mu\text{g mL}^{-1}$  concentrations of  $\text{CaCO}_3$  nanowire. Following the

application of nanowires calcium carbonate, promastigote  $\text{IC}_{50}$  was measured as 800  $\mu\text{g mL}^{-1}$ ; results identified the  $\text{CaCO}_3$  nanowire that have the low toxicity against *L. major*.

## 4. Discussion

In this study, unprecedented synthesis of  $\text{CaCO}_3$  nanowires was accomplished using plant extract. The characterization results of the synthesized nanoparticles confirmed the morphology of nanowires and their star-shaped polycrystalline structures. Schematic of the formation process of the  $\text{CaCO}_3$  nanowire are shown in Fig. 5, nanostring like  $\text{CaCO}_3$  particles with homogeneous size distribution were initially formed and then aggregated and finally the growth of  $\text{CaCO}_3$  nanowires ensued.

Due to the high toxicity of plant physicochemical on *Leishmania* parasite,<sup>47</sup> the use of nanoparticles containing these compounds reduces the medical costs for the disease treatment by minimizing the adverse effects, improving the solubility, without generating cytotoxicity.

Also, the mechanisms for the conventional drug resistance are often associated with lower drug uptake, faster drug metabolism, increased efflux, drug target variations, and the over-expression of drug transporters. The high outbreak rate of CL and the presence of resistance to conventional drugs highlight a demand for promoting and exploring new, low toxic and minimal cost drugs. According to the results of Borrego-Sánchez *et al.*, the solubility of praziquantel antiparasitic drugs with calcium carbonate increased in the acidic medium and cytotoxicity study revealed no cell death in HTC116 cells.<sup>48</sup> Tessarolo *et al.*, showed which benzimidazole delivery with calcium carbonate was more toxic on *Trypanosoma cruzi* compared with benzimidazole alone.<sup>49</sup> One of the biggest





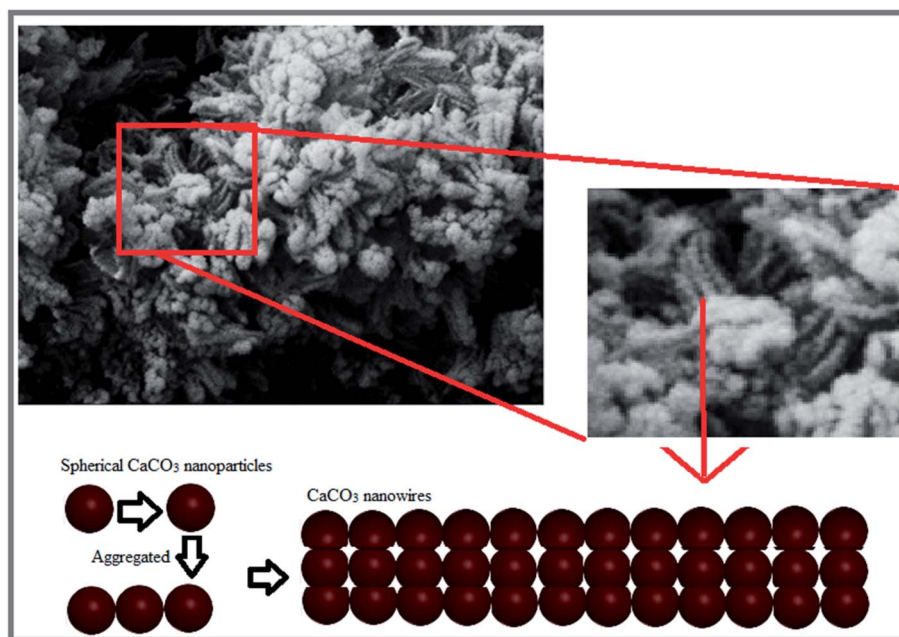


Fig. 5 Schematic of formation process of the  $\text{CaCO}_3$  nanowire.

challenges in treating tropical diseases, as a public health problem, has been its cost. Herein, the  $\text{CaCO}_3$  nanowires were synthesized using an inexpensive method. Additionally, calcium carbonate nanostructures may be used as a smart anticancer drug carrier.<sup>50,51</sup>

## 5. Conclusion

Calcium nanowires were synthesized using a plant extract. Their leishmanicidal effects were evaluated on *Leishmania major* in *in vitro*. These results confirm that the plant extract offer an easy, inexpensive and an effective method to synthesize calcium carbonate nanowires without using any harmful chemicals detrimental to humans and or environment.

## Authors' contributions

The authors read and approved the final manuscript.

## Conflicts of interests

The authors confirm that there are no competing interests.

## Acknowledgements

This work is partially supported by the Bam and Shahid Beheshti Medical Sciences University.

## References

- 1 K. S. Khashan, G. M. Sulaiman, S. A. Hussain, T. R. Marzoog and M. S. Jabir, *J. Inorg. Organomet. Polym. Mater.*, 2020, 1–17.
- 2 M. Safaei, M. M. Foroughi, N. Ebrahimpour, S. Jahani, A. Omidi and M. Khatami, *TrAC, Trends Anal. Chem.*, 2019, **118**, 401–425.
- 3 M. Mostafavi, I. Sharifi, S. Farajzadeh, P. Khazaeli, H. Sharifi, E. Pourseyedi, S. Kakooei, M. Bamorovat, A. Keyhani, M. H. Parizi, A. Khosravi and A. Khamesipour, *Biomed. Pharmacother.*, 2019, **116**, 108942.
- 4 B. Noorani, F. Tabandeh, F. Yazdian, Z.-S. Soheili, M. Shakibaie and S. Rahmani, *Int. J. Polym. Mater. Polym. Biomater.*, 2018, **67**, 754–763.
- 5 M. Khatami, H. Q. Alijani, H. Heli and I. Sharifi, *Ceram. Int.*, 2018, **44**, 15596–15602.
- 6 A. A. L. Sepúlveda, A. M. A. Velásquez, I. A. P. Linares, L. de Almeida, C. R. Fontana, C. Garcia and M. A. S. Graminha, *Photodiagn. Photodyn. Ther.*, 2020, **30**, 101676.
- 7 K. Lubis, N. Chudapongse, H. V. Doan and O. Weeranantanapan, *Curr. Nanosci.*, 2020, **16**, 214–225.
- 8 J. Pavez, J. F. Silva and F. Melo, *Electrochim. Acta*, 2005, **50**, 3488–3494.
- 9 N. H. de Leeuw and S. C. Parker, *J. Phys. Chem. B*, 1998, **102**, 2914–2922.
- 10 Z. Azizi, S. Pourseyedi, M. Khatami and H. Mohammadi, *J. Cluster Sci.*, 2016, **27**, 1613–1628.
- 11 M.-G. Ma, Y.-Y. Dong, L.-H. Fu, S.-M. Li and R.-C. Sun, *Carbohydr. Polym.*, 2013, **92**(2), 1669–1676.
- 12 S. Weiner, Y. Levi-Kalishman, S. Raz and L. Addadi, *Connect. Tissue Res.*, 2003, **44**, 214–218.
- 13 A. G. Turnbull, *Geochim. Cosmochim. Acta*, 1973, **37**, 1593–1601.
- 14 M. S. Rao, *Bull. Chem. Soc. Jpn.*, 1973, **46**, 1414–1417.
- 15 A. Biswas, A. T. Nagaraja and M. J. McShane, *ACS Appl. Mater. Interfaces*, 2014, **6**, 21193–21201.



- 16 M. A. S. Melo, L. Cheng, K. Zhang, M. D. Weir, L. K. Rodrigues and H. H. Xu, *Dent. Mater.*, 2013, **29**, 199–210.
- 17 L. K. Foong, M. M. Foroughi, A. F. Mirhosseini, M. Safaei, S. Jahani, M. Mostafavi, N. Ebrahimipoor, M. Sharifi, R. S. Varma and M. Khatami, *RSC Adv.*, 2020, **10**, 15430–15460.
- 18 S. Maleki Dizaj, M. Barzegar-Jalali, M. H. Zarrintan, K. Adibkia and F. Lotfipour, *Expert Opin. Drug Delivery*, 2015, **12**, 1649–1660.
- 19 X. He, T. Liu, Y. Chen, D. Cheng, X. Li, Y. Xiao and Y. Feng, *Cancer Gene Ther.*, 2008, **15**, 193–202.
- 20 A. Khoshraftar, B. Noorani, F. Yazdian, H. Rashedi, R. Vaez Ghaemi, Z. Alihemmati and S. Shahmoradi, *Int. J. Polym. Mater. Polym. Biomater.*, 2018, **67**, 987–995.
- 21 G.-B. Cai, G.-X. Zhao, X.-K. Wang and S.-H. Yu, *J. Phys. Chem. C*, 2010, **114**, 12948–12954.
- 22 K. Islam, A. Zuki, M. Ali, B. Hussein, M. Zobir, M. Noordin, M. Loqman, H. Wahid, M. Hakim and A. Hamid, *J. Nanomater.*, 2012, **2012**, 1–5.
- 23 H.-D. Yu, Z.-Y. Zhang, K. Y. Win, J. Chan, S. H. Teoh and M.-Y. Han, *Chem. Commun.*, 2010, **46**, 6578–6580.
- 24 K. Fujihara, M. Kotaki and S. Ramakrishna, *Biomaterials*, 2005, **26**, 4139–4147.
- 25 M. Bamorovat, I. Sharifi, M. R. Aflatoonian, B. Sadeghi, A. Shafian, R. T. Oliaee, A. Keyhani, A. A. Afshar, A. Khosravi, M. Mostafavi, M. H. Parizi, M. Khatami and N. Arefinia, *Int. Immunopharmacol.*, 2019, **69**, 321–327.
- 26 M. Bamorovat, I. Sharifi, M. R. Aflatoonian, H. Sharifi, A. Karamoozian, F. Sharifi, A. Khosravi and S. Hassanzadeh, *PLoS One*, 2018, **13**, e0192236.
- 27 M. Bamorovat, I. Sharifi, S. Dabiri, M. A. Mohammadi, M. Fasihi Harandi, M. Mohebbali, M. R. Aflatoonian and A. Keyhani, *Iran. J. Public Health*, 2015, **44**, 1359–1366.
- 28 A. Shokri, M. Fakhar, J. Akhtari and P. Gill, *J. Mazandaran Univ. Med. Sci.*, 2016, **25**, 412–429.
- 29 K. Saleem, Z. Khursheed, C. Hano, I. Anjum and S. Anjum, *Nanomaterials*, 2019, **9**, 1749.
- 30 N. Sattarahmady, A. Rahi and H. Heli, *Sci. Rep.*, 2017, **7**, 11238.
- 31 H. Hossein and N. Masoud, *Recent Pat. Nanotechnol.*, 2017, **11**, 1–12.
- 32 M. Khatami, I. Sharifi, M. A. L. Nobre, N. Zafarnia and M. R. Aflatoonian, *Green Chem. Lett. Rev.*, 2018, **11**, 125–134.
- 33 T. Iranmanesh, M. M. Foroughi, S. Jahani, M. Shahidi Zandi and H. Hassani Nadiki, *Talanta*, 2020, **207**, 120318.
- 34 Z. U. H. Khan, A. Khan, Y. M. Chen, N. S. Shah, A. U. Khan, N. Muhammad, K. Tahir, H. U. Shah, Z. U. Khan, M. Shakeel, M. Nadeem, M. Imran and P. Wan, *J. Photochem. Photobiol., B*, 2018, **180**, 208–217.
- 35 H. Singh, J. Du, P. Singh and T. H. Yi, *J. Nanostruct. Chem.*, 2018, **8**, 359–368.
- 36 S. Nozohouri, R. Salehi, S. Ghanbarzadeh, K. Adibkia and H. Hamishehkar, *Mater. Sci. Eng. C*, 2019, **99**, 752–761.
- 37 M. Khatami, S. Irvani, R. S. Varma, F. Mosazade, M. Darroudi and F. Borhani, *Bioprocess Biosyst. Eng.*, 2019, **42**, 2007–2014.
- 38 S. Azhdari, R. E. Sarabi, N. Rezaeizade, F. Mosazade, M. Heidari, F. Borhani, M. Abdollahpour-Alitappeh and M. Khatami, *RSC Adv.*, 2020, **10**, 29737–29744.
- 39 M. Darroudi, M. Bagherpour, H. A. Hosseini and M. Ebrahimi, *Ceram. Int.*, 2016, **42**, 3816–3819.
- 40 L. Pérez-Villarejo, F. Takabait, L. Mahtout, B. Carrasco-Hurtado, D. Eliche-Quesada and P. J. Sánchez-Soto, *Ceram. Int.*, 2018, **44**, 5291–5296.
- 41 M. E.-S. I. Saraya and H. Rokbaa, *Am. J. Nanomater.*, 2016, **4**, 44–51.
- 42 M. Ghiasi and A. Malekzadeh, *Cryst. Res. Technol.*, 2012, **47**, 471–478.
- 43 T. Schöler and W. Tremel, *Chem. Commun.*, 2011, **47**, 5208–5210.
- 44 S. Donatan, A. Yashchenok, N. Khan, B. Parakhonskiy, M. Cocquyt, B.-E. Pinchasik, D. Khalenkow, H. Möhwald, M. Konrad and A. Skirtach, *ACS Appl. Mater. Interfaces*, 2016, **8**, 14284–14292.
- 45 A. Butt, S. Ejaz, J. Baron, M. Ikram and S. Ali, *Dig. J. Nanomater. Biostructures*, 2015, **10**(3), 799–809.
- 46 S. S. Bari and S. Mishra, *Carbohydr. Polym.*, 2017, **169**, 426–432.
- 47 A. R. Silva, R. Scher, F. V. Santos, S. R. Ferreira, S. C. Cavalcanti, C. B. Correa, L. L. Bueno, R. J. Alves, D. P. Souza and R. T. Fujiwara, *Molecules*, 2017, **22**, 815.
- 48 A. Borrego-Sánchez, R. Sánchez-Espejo, B. Albertini, N. Passerini, P. Cerezo, C. Viseras and C. I. Sainz-Díaz, *Pharmaceutics*, 2019, **11**, 533.
- 49 L. D. Tessarolo, C. P. Mello, D. B. Lima, E. P. Magalhães, E. M. Bezerra, F. A. M. Sales, I. L. B. Neto, M. de Fátima Oliveira, R. P. dos Santos and E. L. Albuquerque, *Parasitology*, 2018, **145**, 1191–1198.
- 50 D. Sun, H. Peng, S. Wang and D. Zhu, *Nanoscale Res. Lett.*, 2015, **10**, 948.
- 51 C. Wang, C. He, Z. Tong, X. Liu, B. Ren and F. Zeng, *Int. J. Pharm.*, 2006, **308**, 160–167.

